ELSEVIER

Chemical Physics 245 (1999) 1–16

Chemical Physics

www.elsevier.nl/locate/chemphys

Third-order microscopic nonlinearities of very long chain polyenes: saturation phenomena and conformational effects

I. Ledoux [a,*], I.D.W. Samuel [a,1,2], J. Zyss [a,3], S.N. Yaliraki [b], F.J. Schattenmann [b], R.R. Schrock [b], R.J. Silbey [b]

[a] *Laboratoire de Photonique Quantique et Moléculaire, UMR 8537, École Normale Supérieure de Cachan, 61 avenue du Président Wilson, F-94235 Cachan Cedex, France*

[b] *Department of Chemistry and Center for Material Science and Engineering, Massachusetts Institute of Technology, Cambridge, MA 02139, USA*

Received 20 January 1999

Abstract

Using the living cyclopolymerization of diethyldipropargylmalonate, very long polyenes (up to 1100 carbon–carbon double bonds) are now available. Molecular masses of these polyenes are determined using the MALDI-TOF technique. Third-order polarizabilities γ of polyene-like molecules with very long conjugation length (N up to 1100 carbon–carbon double bonds) are measured using third-harmonic generation at 1.9 μm in THF solutions. γ values saturate around $N = 60$ double bonds. Modelization of the dependence of γ with respect to N is based on a representation of a conjugated chain as a collection of planar segments separated by large angular breaks. A very good quantitive agreement between calculated and experimental data, both in terms of saturation length and γ/N values is clearly demonstrated.

1. Introduction

Conjugated polymers have interesting and potentially important electrical and optical properties, such as high conductivity when oxidized [1], electroluminescence [2,3], and large non-linear optical susceptibilities [4–7]. The prototype of such conjugated polymer molecules are the polyenes, ranging from small molecules such as hexatriene [8], octatetraene [9] to carotenes [10] and finally polyacetylene. Because of their relative simplicity, these molecules have been the focus of much experimental and theoretical work. The optical properties of short polyenes have been experimentally studied in a series of early papers by Kohler and co-workers [11], and those of polyacetylene by Heeger et al. [12] and Shank et al. [13]. Intermediate-sized molecules have been rarely studied because of the difficulty in synthesis and their instability.

Theoretical studies of the electronic structure and spectra of short polyenes have been carried out by a

* Corresponding author. Previously at C.N.E.T. France Télécom 196, avenue Henri Ravera, F-92220 Bagneux, France. Fax: +33-14705567.

[1] Previously at C.N.E.T. France Télécom 196, avenue Henri Ravera, F-92220 Bagneux, France.

[2] Present address: Dept. of Physics - University of Durham, South Road Durham DH1 3LE - U.K.

[3] Previously at C.N.E.T. France Télécom 196, avenue Henri Ravera, F-92220 Bagneux, France.

0301-0104/99/$ - see front matter
PII: S0301-0104(99)00146-9

number of workers using a variety of semi-empirical methods ranging from the Hückel model (i.e., non-interacting π electrons) [14,15] to the PPP model (interacting π electrons including extended interactions) [16–18]. While the fully interacting model gives an excellent description of the main features of the electronic structure, it is difficult to carry out for systems larger than $\sim$ 10–20 double bonds, and can be used only for particular geometries (e.g., planar all *trans*). The Hückel model can, of course, be solved for any size and any geometry in a rather straightforward, albeit tedious manner. However, one can only expect qualitative results from this approach. These considerations have led to the polyenes becoming a laboratory for studying one-dimensional systems, both theoretically and experimentally.

Ideally, we would like to study the evolution of the optical and electronic properties as a function of the number of double bonds. Unfortunately, this has been hampered by the inability to synthesize polyene oligomers of known size and good solubility, the latter property being important in order to study the single molecule properties, independent of the intermolecular interactions that occur in films, and which are absent in almost all theoretical studies.

Recently, remarkable progress in synthesis has led to the discovery of routes to soluble polyenes with double bonds numbering from $\sim$ 25 to $>$ 1000 [19–21]. With these molecules in hand, we can now study the evolution of properties with N, the number of double bonds. We recently reported [22] the first demonstration of the saturation of the third-order non-linear optical susceptibility, γ, with increasing N.

Comparison of experiment and theory is difficult because most theoretical studies have been limited to planar all *trans*-polyenes, while the molecules in solution will be 'disordered', in the sense that there will be conformational twists around the single bonds in the structure leading to changes in electronic structure and loss of conjugation. There are two limiting theoretical models for this effect: (1) relatively few, strongly disruptive twists leading to a picture of fully conjugated segments of shorter length [23], and (2) relatively many, weakly disruptive twists leading to a worm-like chain [24]. The concept of conjugation length can then be defined for both theoretical models. From theory, we know that, in the case of planar all-*trans* chains, there is a *saturation length* N_s, at which an optical property, for example, becomes proportional to N [25–28]. Thus, for γ, all-*trans* chains longer than N_s, $\gamma = N\{\gamma(N_s)/N_s\} = \gamma(N_s)\{N/N_s\}$, so that the chain acts like N/N_s segments of a chain of length N_s. For real chains with imperfections (twists), we may define a conjugation length by comparison to the perfect all-*trans* chain; that is, a real chain of length N may have the properties of N/N_c segments of all-*trans* chains of length N_c ($N_c < N_s$). A more likely realization is that an ensemble of real chains of length N will have the properties of a probability distribution $P^N(L)$ of all-*trans* chains of varying length, L. Depending on the theoretical model one chooses (worm-like coil or disruptive twists), one will find a different $P^N(L)$.

In the present paper, we investigate two series of long polyene oligomers. The first series has between 14 and 140 double bonds; the second series between 118 and 1190 double bonds. Third-harmonic generation is used to determine their third-order polarizability γ. This technique has the advantage over other methods, like four-wave mixing, to be a zero-background measurement, not hampered by any other processes. In particular, this method precludes any non-electronic (e.g., thermal) contribution to the measured γ values. In addition, we present theoretical studies on long chains to investigate the effects of disorder on the optical properties, such as γ and the linear absorption.

2. Experimental

2.1. Molecules

We recently reported [22] measurements of the third-order hyperpolarizability (γ) of polyenes prepared by the cyclopolymerization of diethyldipropargylmalonate (DEDPM) in a living manner employing initiators of the type $\{(DME)[(CF_3)_2MeCO]_2(NAr)Mo{=}CH\}_2$-1,4-$C_6H_4$ (**1**); Ar = 2,6-*i*-$Pr_2C_6H_3$; DME = 1,2-dimethoxyethane) [20]. Such polymers contain a random mixture of 5- and 6-membered rings that are formed as a consequence of α or β addition (Scheme 1) of the first triple bond to the initial and intermediate Mo=C bonds (Series I). (Five- and six-membered rings can be distinguished

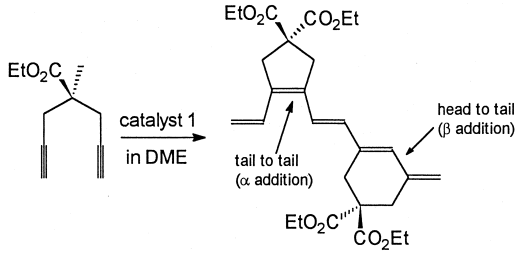

Scheme 1.

easily from one another by the chemical shift of the quaternary carbon in the ring [21].) The number average molecular weight of such polyenes was determined by viscometry vs. a polystyrene standard and found to be significantly higher than that predicted on the basis of the number of monomers added, even though the polydispersity was found to be low (~ 1.10, see Table 1). Values for γ were correlated with the average number of double bonds in the chain assuming the molecular weight to be that determined by viscometry. (Light scattering was not possible, as these polymers absorb at 690 nm, the wavelength of the laser employed in the light scattering detector.)

Diethyldipropargylmalonate was found to be cyclopolymerized by initiator $(Ph_3CO_2)_2$(*N*-2-*t*-BuC_6H_4)Mo=CH-*t*-Bu (**2**) in a living fashion to give a polymer that contains almost exclusively 6-membered rings [29]. The molecules are similar to those of Series I, but without the central phenyl ring, and with all 6-membered rings instead of a mixture of 5- and 6-membered rings (Fig. 1). The polymers made with initiator **2** (containing up to 20 equivalents of monomer, Series II) again were found to have a molecular weight higher than expected by viscometry, although again a polydispersity between 1.10 and 1.15. Polymers (Series III) that contain only 6-membered rings were also prepared using Mo(*N*-adamantyl)$(CHCMe_2Ph)(O_2CPh_3)_2$ (**3**) [30]. Molecular weights were determined using light scattering (620 nm; Wyatt Technologies) in THF. Molecular weights found by light scattering are more than $10\times$ the predicted value, as a consequence of a large ratio of the rate of propagation to the rate of initiation. These findings are consistent with the observed relatively large polydispersities, usually 1.5–1.7.

NLO measurements were performed on Series III also in order to correlate γ with the average number of double bonds in the chain and with the structure of the backbone of the polymer.

In order to determine the average molecular weight accurately for polymers prepared employing **1** and **2**, we explored the possibility of using MALDI-TOF mass spectrometry. MALDI-TOF mass spectrometry has only recently been employed for the characterization of synthetic polymers [31–36]. This 'soft' ionization technique allows the detection of the individual masses of chains within a distribution of polymers, as long as the polymer has a relatively low molecular weight. Spectra were obtained for five samples containing from 5 to 20 monomers on the average that had been characterized by GPC/viscometry. A representative spectrum (of the 5-mer) is

Table 1
GPC and MALDI/TOF MS[a] data for poly(DEDPM) prepared using initiators **1** and **2**[a]

Polymer	Initiator	M_n(calc.)	M_n(V)[b]	PDI(V)[b]	M_n(M)[c]	PDI(M)[c]	M_n(V)/M_n(M)
$(DEDPM)_5$	2	1342	6847	1.18	2810	1.09	2.4
$(DEDPM)_8$	2	2050	7105	1.22	3270	1.11	2.2
$(DEDPM)_{11}$	2	2759	9452	1.26	3730	1.14	2.5
$(DEDPM)_{15}$	2	3704	11500	1.26	4960	1.13	2.3
$(DEDPM)_{20}$	2	4886	13590	1.26	5470	1.15	2.5
$(DEDPM)_6$	1	1700	2800	1.19	1760	1.09	1.6
$(DEDPM)_{15}$	1	3826	5400	1.14	2960	1.11	1.8

[a] Details concerning the polymerization conditions can be found in Ref. [29] (for **2** = Mo(*N*-3-*t*-BuC_6H_4)$(CHCMe_3)(O_2CPh_3)_2$) and Ref. [20] (for **1** = {Mo(*N*-2,6-*i*-$Pr_2C_6H_4$)BuC_6H_4][$OCMe(CF_3)_2$]$_2$}$_2$(1,4-4CH)).
[b] Determined by GPC on-line viscometry (V) vs. a polystyrene universal calibration curve (Viscotek).
[c] Determined by MALDI/TOF mass spectroscopy (M).

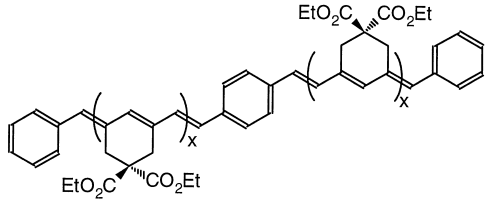

and

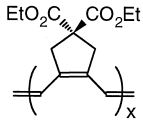

Series I

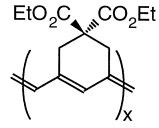

Series II and III

Fig. 1. Chemical structures of Series I, II and III molecules.

shown in Fig. 2. $M_{n,}$ M_w, and PDI were determined by using the peak height as an approximation for n_i, the number of chains with length i, assuming that the distribution observed is virtually identical to the distribution in the matrix.

M_n, M_w, and PDI respectively are defined as

$$M_n = \frac{\sum n_i M_i}{\sum n_i},$$

$$M_w = \frac{\sum n_i M_i^2}{\sum n_i M_i},$$

and

$$\mathrm{PDI} = \frac{M_w}{M_n}.$$

MALDI spectra in which the signal to noise ratio was relatively high could be obtained only on polymers containing 20 equivalents of DEDPM or less per equivalent of **2**. Spectra of higher molecular weight polymers (40-mer and up) exhibited a signal to noise ratio too low to allow a reliable determination of polydispersities and molecular weights.

The mass difference between individual signals is 236, which is the mass of a single monomer. Therefore only monocations are formed. The molecular weight of each individual peak in fact is that expected, if one includes the end groups from the initiator and from the quenching process with benzaldehyde (benzylidene). For example, the labeled peak in Fig. 2 has M_n(found) = 1814.7 and an M_n(calc) = 1814.2. The pattern of peaks of lower intensity in Fig. 2 differs by $\sim$90 units from the higher intensity pattern. The origin of this polymer distribution is still unknown.

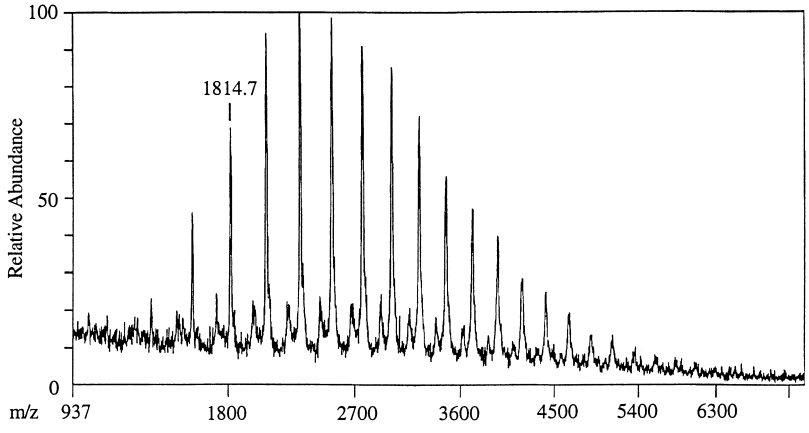

Fig. 2. MALDI-TOF mass spectrum of $(DEDPM)_5$ prepared by employing initiator **2**.

The data obtained by MALDI show a linear correlation with the amount of monomer added (Table 1). However, the M_n values determined by MALDI are smaller by a factor between 2.2 and 2.5 than those determined by GPC viscometry. However, the value for M_n determined by MALDI is still larger than M_n(calc). (The ratio of $M_n(M)/M_n$(calc) decreases from ~ 2 for the 5-mer to ~ 1.1 for the 20-mer.) Therefore the rate of propagation is not much larger than the rate of initiation. Therefore the polydispersities lie in the range around 1.10. The discrepancy between the M_n values determined by MALDI and by viscometry can be attributed to different solution properties of the conjugated polymers compared to polystyrene, in particular a likely more rigid rod-like structure instead of a random coil. Since the ratio of M_n values obtained by viscometry vs. values obtained by MALDI was found to be relatively constant over the entire range (from five to twenty monomers), we feel comfortable applying a conversion factor of 2.40 to the M_n values determined by viscometry for poly(DEDPM) prepared using **2** as an initiator. Alternatively, we can construct a calibration curve (M_n vs. number of monomers) that would allow us to determine the value of M_n. For polymers longer than a 20-mer the average molecular weight can be assumed to be approximately that predicted on the basis of the number of monomers added to the initiator.

A significant question is whether the M_n values determined by viscometry for poly(DEDPM) that contains a statistical mixture of 5- and 6-membered rings (prepared using initiator **1**) are also high by a factor of ~ 2. Two samples on which NLO measurements were made previously [22] were examined by MALDI and shown to have M_n values (Table 1) lower by a factor of 1.7 compared to the M_n values obtained by viscometry. The exact 'conversion' factor depends, as it should, on the exact structure of the polymer under consideration. On the basis of the limited amount of data we have in hand for poly(DEDPM) (Table 1) the value for M_n calculated on the basis of the number of monomers added is approximately the correct molecular weight, consistent with a rate of initiation that is approximately the same as the rate of propagation and slightly lower polydispersities for these samples. Therefore, we have applied for molecular masses and conjugation lengths in Series I a reduction factor of 1.7 with respect to data reported in Ref. [22]. As a consequence, γ and $\gamma(0)$ values have to be divided by the ratio $M_n(V)/M_n(M)$.

2.2. Nonlinear optical measurements

The cubic nonlinearity γ of the molecules of Series I and III was measured by third-harmonic generation in tetrahydrofuran (THF) solution. A wedge-shaped solution cell was translated across the excitation beam, and the resulting Maker fringes were measured and analysed as previously described [22]. Excitation at 1907 nm was provided by a hydrogen Raman-shifted Q-switched Nd^{3+}:YAG laser, so that the third-harmonic signal at 636 nm was just below the onset of the absorption of the molecules. The excitation intensity was of order 100 MW/cm^2. The solutions were of concentration in the range 10^{-6}–10^{-3} M, and towards the lower end of this range for the longer molecules. The measurements were made relative to pure THF, which was taken to have a nonlinearity of 1.48×10^{-36} esu.

We also looked at the stability of a representative molecule – the 30-mer. We measured the γ immediately after preparing the solution in THF, then several times during the following six hours, and finally four days later. We find that the measurements on the day of preparation of the solution are not significantly different from one another, but that after 4 days, the signal has fallen to approximately one-third. Usually we measure the γ of solutions within 1 h of preparation, so that degradation of the molecules is not a problem.

3. Results

3.1. UV–Vis absorption spectra

The data for the molecules in Series I are summarised in Table 2. The molecules show a fairly broad absorption in the visible region of the spectrum due to π–π^* transitions. The position of the peak of the absorption (λ_{max}) shifts to longer wavelength as the chainlength increases, although the position of λ_{max} for the longest molecule in this

Table 2
Maximum absorption wavelength λ_{max}, 'effective' conjugation length N_{eff}, cubic hyperpolarizabilities values $\gamma(-3\omega;\omega,\omega,\omega)$ as measured by THG at 1.9 μm and their corresponding 'static' $\gamma(0;0,0,0)$ values, $\gamma(-3\omega;\omega,\omega,\omega)/N$ and $\gamma(0;0,0,0)/N$, for polyenes with N conjugated double bonds polymerized with initiator **1** (Series I)

N[c]	Molecular mass	PDI	λ_{max} in THF (nm)	N_{eff} (THF)	$\gamma(-3\omega;\omega,\omega,\omega)$ (10^{-34} esu)	$\gamma(0;0,0,0)$ (10^{-34} esu)	$\gamma(-3\omega;\omega,\omega,\omega)/N$ (10^{-34} esu)	$\gamma(0;0,0,0)/N$ (10^{-34} esu)
14	1760[a]	1.19	466	9.05	51	23	3.64	1.64
20	2412[b]	1.16	486	10.3	83	32	3.65	1.6
25	2960[a]	1.14	516	12.8	135	43	5.4	1.73
35	4412[b]	1.14	530	14.3	325	90	8.5	2.37
50	5883[b]	1.14	538	15.3	603	157	12.0	3.14
88	10353[b]	1.19	550	16.9	1600	370	18.2	4.2
140	16412[b]	–	552	17.3	2232	503	15.9	3.6

[a] Values found by MALDI (see Table 1).
[b] M_n determined by viscometry vs. polystyrene and converted using a factor of 1.7.
[c] Calculated from the molecular mass.

series ($N = 140$) is well short of the λ_{max} of polyacetylene films. For Series III, the absorption spectrum is broader than for the molecules in Series I or II, consistent with the larger PDI values. This introduces some imprecision into the estimation of λ_{max}. Nevertheless λ_{max} tends to increase with chainlength, although the dependence on chainlength for Series III is weaker than in Series I (see Table 3). Even though the molecules of Series III are longer than those of Series I, the wavelength of the maximum of their absorption is shorter.

We have introduced in Tables 2 and 3 the 'effective conjugation length' N_{eff}, according to the formula usually used to describe the relationship between the number of double bonds and the energy E_n of the first electronic transition of an all-*trans* 'ideal' polyene containing N double bonds [37]:

$$E_n = E_\infty + k/N_{eff},$$

where E_∞ is the HOMO–LUMO gap of a hypothetical infinite polyene. Parameters E_∞ and k are inferred from a fit of the form $E = A + B/N$ to exper-

Table 3
Maximum absorption wavelength λ_{max}, 'effective' conjugation length N_{eff}, cubic hyperpolarizabilities values $\gamma(-3\omega;\omega,\omega,\omega)$ as measured by THG at 1.9 μm and their corresponding 'static' $\gamma(0;0,0,0)$ values, $\gamma(-3\omega;\omega,\omega,\omega)/N$ and $\gamma(0;0,0,0)/N$, for polyenes with N conjugated double bonds, for molecules polymerized with initiator **3** (Series III)

Name	Molceluar mass	PDI	N	λ_{max} in THF (nm)	N_{eff} (THF)	$\gamma(-3\omega;\omega,\omega,\omega)$ (10^{-34} esu)	$\gamma(0;0,0,0)$ (10^{-34} esu)	$\gamma(-3\omega;\omega,\omega,\omega)/N$ (10^{-34} esu)	$\gamma(0;0,0,0)/N$ (10^{-34} esu)
3-mer	16360	1.21	137	480	9.9	336	134	2.45	0.98
5-mer	14030	1.31	118	488	10.5	288	110	2.44	0.93
7-mer	19370	1.47	163	492	10.8	300	113	1.84	0.69
9-mer	18450	1.63	156	497	11.2	432	156	2.77	1.00
11-mer	21010	1.71	177	493	10.8	456	170	2.57	0.96
14-mer	24630	1.69	208	500	11.4	432	154	2.07	0.74
20-mer	43060	1.63	364	498	11.2	912	336	2.50	0.92
30-mer	65070	1.51	550	505.5	11.9	1656	577	3.01	1.05
45-mer	58000	2.09	491	497	11.2	1608	576	3.27	1.17
65-mer	103900	1.62	880	507	12.0	2760	936	3.13	1.06
90-mer	109600	1.74	928	510	12.3	2244	744	2.42	0.80
125-mer	122700	1.80	1039	511	12.4	3360	1104	3.23	1.06
200-mer	140500	1.77	1190	510	12.3	3840	1272	3.23	1.07

[a] Initiator = Mo(*N*-adamantyl)(CHCMe$_2$Ph)(O$_2$CPh$_3$)$_2$ (**3**) [30].

imental transition energies of 'model' short polyenes ($N < 16$) in THF [6]: $E_\infty = 1.79$ eV and $k = 7.88$. In both cases, N_{eff} is much weaker than the 'nominal' N values, the highest discrepancy occurring for the highest N values, especially in Series III.

Transition energies E are plotted with respect to $1/N$ for Series I (Fig. 3a) and Series III (Fig. 3b) in two different solvents. UV–Vis spectra appear to be slightly more sensitive to solvent effects in the case of Series III. In both series (THF solution), the relationship $E_N = E_\infty + k/N$ [37] is fully valid, the values of E_∞ being 2.15 and 2.43 eV for Series I and III, respectively. These values remain far from $E_\infty =$ 1.79 eV as inferred from UV–Vis spectra of all-*trans* 'model' polyenes in THF [6], Series III exhibiting the highest E_∞ value.

3.2. Hyperpolarizabilities

For Series I, we find that the γ of these molecules increases with chainlength, reaching a giant value of $(2200 \pm 250) \times 10^{-34}$ esu for 140 double bonds. This value is one thousand times larger than would be expected for non-conjugated molecules of a similar size, and a factor of 20 larger than the previously reported γ for $N = 16$ [6]. The dependence of the cubic nonlinearity per repeat unit, γ/N, on chain-length is shown in Fig. 4. It is clear that there is a

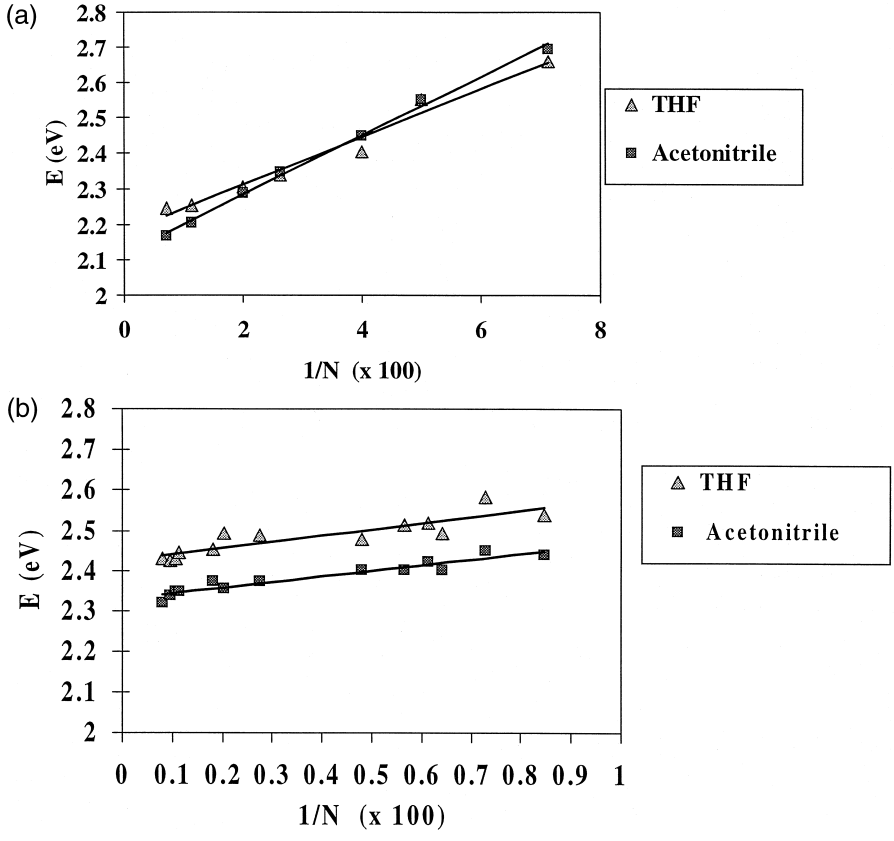

Fig. 3. (a) Plot of the HOMO–LUMO transition energy E with respect to $1/N$, where N is the number of conjugated double bonds, for Series I, in THF and acetonitrile. In both cases, a linear behavior is observed, described by the following relations: E_N (in eV) $= 5.93/N +$ 2.15 in THF, E_N (in eV) $= 7.29/N + 2.09$ in acetonitrile. (b) Plot of the HOMO–LUMO transition energy E with respect to $1/N$, where N is the number of conjugated double bonds, for Series III, in THF and dichloromethane. In both cases, a linear behavior is observed, described by the following relations: E_N (in eV) $= 6.32/N + 2.43$ in THF, E_N (in eV) $= 5.79/N + 2.33$ in acetonitrile.

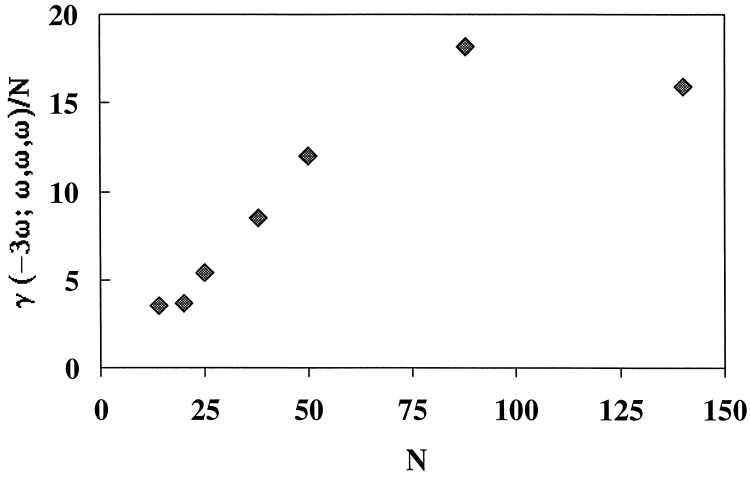

Fig. 4. Plot of $\gamma(-3\omega;\omega,\omega,\omega)/N$ (in 10^{-34} esu) with respect to the number N of double bonds for Series I. γ is measured by third-harmonic generation in THF at 1.91 μm.

saturation of the increase of γ/N with chainlength. γ/N increases with N for the shorter molecules, but reaches a value that is constant (within the experimental error) for the longest molecules. The onset of the saturation occurs at around 60 double bonds.

We have estimated at zero frequency (see Table 2) using a model with a one-photon transition at hc/λ_{max} above the ground state, and with two-photon allowed states far from resonance:

$$(0;0,0,0) = \left[1-(\lambda_{max}/\lambda)^2\right]\left[1-(3\lambda_{max}/\lambda)^2\right] \times \gamma(-3\omega;\omega,\omega,\omega),$$

where $\lambda = 1907$ nm is the excitation wavelength. The saturation behaviour of $\gamma(0;0,0,0)$ and $\gamma(-3\omega;\omega,\omega,\omega)$ is very similar.

This saturation is also very clear in a plot of $p = [\mathrm{d}\ln\gamma]/[\mathrm{d}\ln N]$ vs. chainlength (Fig. 5). In the case of a simple power-law dependence of γ on chainlength $\gamma = kN^a$, p would have a constant value of a. The observed behaviour is far more complicated, with a maximum of p for $N = 35$. p then decreases, which corresponds to $\gamma \propto N$ (saturation) for the longest molecules. This variation of p with chainlength shows that our data cannot be described by a simple power law.

We have estimated the macroscopic cubic susceptibility $\chi^{(3)}$ corresponding to the value of γ/N we measure in the longest molecules of Series I. Assuming the same packing density (3×10^{14} cm^{-2}) and local field factor (10) as for polyacetylene gives $\chi^{(3)} \sim 2\times10^{-10}$ esu (0.5×10^{-10} esu after correction to zero frequency). This value is similar to the experimental value in oriented polyacetylene of $(4\pm2)\times10^{-10}$ esu at 1064 nm reported by Sinclair et al. [38] after allowing for the effects of resonance (which could enhance Sinclair's value by a factor of 2 to 3) and orientation (which could give an enhancement of up to a factor of 5). Larger values of $\chi^{(3)}$ have been reported at resonance [39]. There is a large uncertainty in our estimate of $\chi^{(3)}$, and so we consider it to be in satisfactory agreement with theoretical calculations of $\chi^{(3)}$ of 2×10^{-10} esu at zero frequency [40,41].

The results of measurements on Series III, which consists of longer molecules, are summarised in Table 3 and shown in Fig. 6. The graph shows that γ is proportional to N (i.e., that γ/N is constant within the experimental error). This saturated behaviour throughout this series of molecules with 118–1190 double bonds is entirely consistent with the saturated behaviour for $N > 50$ double bonds seen for Series I. However, the value of γ/N (3×10^{-34} esu) at saturation in Series III is less than

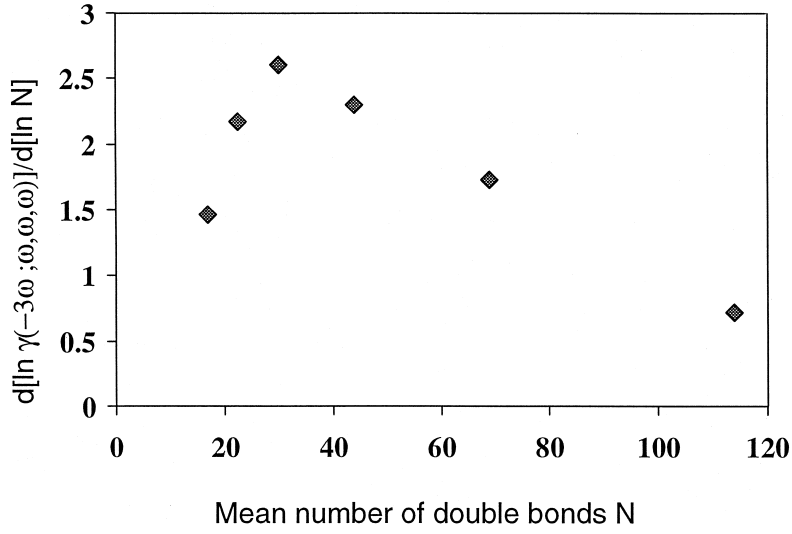

Fig. 5. Plot of $d[\ln \gamma(0)]/[d \ln N]$ with respect to N as deduced from NLO data on Series I molecules.

one-fifth of the value of γ/N (17.10^{-34} esu) for Series I. This discrepancy is significantly reduced when considering $\gamma(0;0,0,0)/N$ values instead of $\gamma(-3\omega;\omega,\omega,\omega)$, but remains large (by a factor >3). The value of $\chi^{(3)}$ for Series III will be smaller by the same factor. We have estimated $\gamma(0;0,0,0)$ in the same way as for Series I, and find that this makes no difference to the saturation behaviour. It may be noted that for similar N_{eff} values, the discrepancy on $\gamma(0)/N$ values between Series I and Series III does not exceed 50%: for $N_{\text{eff}} \approx 12.5$, $\gamma(0)/N = 1.87 \times 10^{-34}$ esu for Series I ($N = 30$)

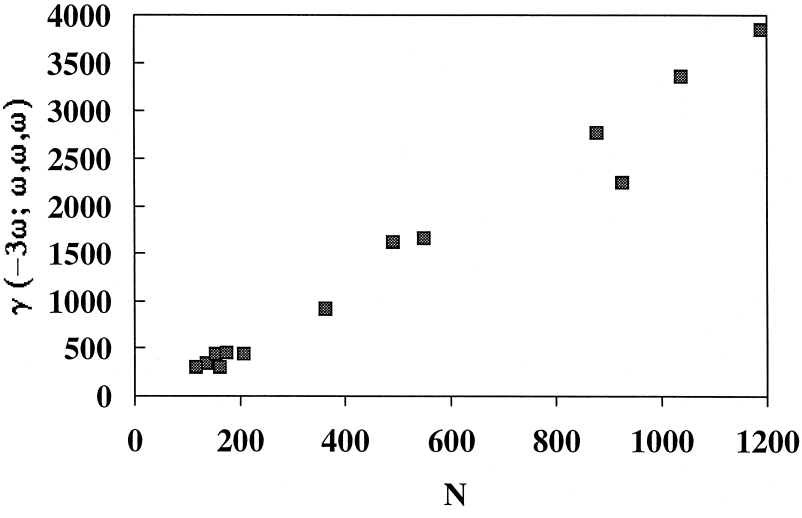

Fig. 6. Chainlength dependence of $\gamma(-3\omega;\omega,\omega,\omega)$ (in 10^{-34} esu) for Series III. γ is measured by third-harmonic generation in THF at 1.91 μm. A linear dependence is clearly observed.

and $\gamma(0)/N = 1.07 \times 10^{-34}$ esu for Series III (200-mer); for $N_{\text{eff}} \approx 10.3$, $\gamma(0)/N = 1.6 \times 10^{-34}$ esu for Series I ($N = 20$) and $\gamma(0)/N = 0.92\ 10^{-34}$ esu for Series III (5-mer).

4. Modelling

4.1. Presentation

We study the conformational behavior of a conjugated polyene chain with allowed rotations around the single bonds. Here, we take into account the electronic transfer and steric repulsion interactions of the system as the most relevant to our purpose. It is widely accepted that, due to steric interactions, the delocalization of electrons is hindered [42–46]. The manner and extent of this is yet to be fully understood. We propose that the chain distorts in a fashion to form numerous almost planar segments, separated by local breaks (or 'flips') caused by large relative angles. Specifically, a number of consecutive double bonds are nearly coplanar with those adjacent until the following one lies in a plane forming an angle of much greater magnitude than the previous ones. Then we expect its adjacent double bonds to form another planar segment until a further flip occurs. We thus expect a distribution of angles between double bonds mainly concentrated around zero, occurring in clusters, with a few outside of that range.

To substantiate the proposed picture, we calculate the probability distribution of such breaks, as well as the number and length of planar segments in a chain of total $2N$ carbon atoms. We compare the results with numerical experiments of the same systems. The agreement is very good. We then compute the third-order polarizability γ of such a conjugated system and compare to experiment [21,22]. The chain behaves in effect, not as one of smaller than original length, but as a collection of smaller ones. In this study we neglect interactions among those segments. Also, the length of these segments may not be constant, but may change together with the configuration of the chain with time evolution. A chain of $2N$ atoms with one unpaired electron per atom is considered. The chain is treated as a one-dimensional system with $2N$ sites, each occupied by an atom. The most relevant interactions for our problem are the steric and solvent interactions between adjacent groups, which tend to keep adjacent double bonds away from planarity, and the delocalization of electrons, which favors the planar conformation. The electron–phonon coupling interaction is explicitly neglected, although bond dimerization is imposed. Electron–electron interactions are not considered at this stage. We expect that, to lower electron repulsion, they reduce delocalization, thus making the steric effect even more important and our picture more relevant. The Hamiltonian

$$H = -\sum_{\sigma,n=1}^{N} \left[t_{\text{d}} c^{*}_{n\sigma,1} c_{n\sigma,2} + t_{\text{s}} \cos(\theta_n - \theta_{n+1}) \times c^{*}_{n\sigma,2} c_{(n+1)\sigma,1} + \text{h.c.} \right] + \sum_{n=1}^{N} V_0 \cos(\theta_n - \theta_{n+1})$$

describes the conjugation and the steric effect. Each of the N unit cells contains two carbon atoms – a double and a single bond of fixed length. The standard fermionic operators $c^{*}_{n\sigma,\text{a}}$ ($c^{*}_{n\sigma,\text{a}}$) create (annihilate) an electron of spin σ on position a of unit cell n. t_{s} and t_{d} are the electron transfer integrals for single and double bonds, respectively. They can be obtained from experimental observation of the band gap in the usual manner [47,48]. Notice that transfer across a single bond depends on the relative orientation of the neighbouring double bonds. V_0 represents an effective steric hindrance energy parameter. If the interaction is favorable, as for example in hydrogen bonding cases, the negative sign is appropriate; if the steric interactions are repulsive, then we can consider a term of the form $\cos(\pi - \phi) = -\cos(\phi)$. The physical picture of the angles is the same, but a negative sign appears, so the sign is in fact irrelevant.

Our model stresses the competition between conjugation (energy E_{c}) and steric interactions (energy E_{s}). As such it is related to that of Rossi et al. [49] We should emphasize that we begin from a microscopic description instead of using the phenomenological Hamiltonian of Rossi et al. [49]:

$$H_{\text{R}} = \sum_{n=1}^{N} \left\{ -E_{\text{c}} \cos 2(\theta_n - \theta_{n+1}) - E_{\text{s}} \cos 2(\theta_n - \theta_{n+1}) \right\} = H_{\text{conj}} + H_{\text{ster}}\,.$$

The form of the conjugation term complies with our intuitive understanding: it exhibits a minimum when the double bonds are aligned, and a maximum when they are perpendicular to each other. By a simple change of variables $\phi_n = \phi_n - \phi_{n+1}$, with Jacobian equal to unity, we can transform both Hamiltonians to variables, ϕ_i, relative angle of double bonds.

Through a perturbation expansion for small angles starting from the electronic part of our model (Scheme 1), we have derived a $\cos 2\theta$ dependence for the conjugation energy and relate it analytically to the ratio of transfer integrals [23]. We have also shown numerically not only agreement with the E_c value, but also with the $\cos 2\theta$ functional dependence. We find the conjugation energy to be [$t = t_d/t_s$], for values of t not far from unity:

$$E_c = \{t_s/4\pi\}\Big[\{\ln 4 + 2\coth^{-1}(t)/(1+t)\} + 2t^2\big(\ln 4 + 2\coth^{-1}(t)\big) - t(l+t)^2\Big].$$

We notice immediately the dependence of the conjugation energy per units of t_d on the ratio, t, of the transfer integrals. According to standard mean field theories [49], we can show that this ratio depends only on the band gap and band width of the system-readily measurable properties: $t_d/t_s = \{1 + E_g/W_g\}/\{1 - E_g/W_g\}$, where E_g stands for the band gap and W_g for the band width of the system. We are thus able to connect our microscopic model to a phenomenological one whose parameters can be obtained from experimental data. By using approximate values for $E_g = 1.4$ eV and $W_g = 10$ eV from the literature, we obtain $E_c/N = 0.015$ eV. To check the validity of our approximations, we performed numerically the same calculation with the original electronic Hamiltonian, and obtained the same value for E_c. Having made the above connections, we can use H_R to study the chain with conformational disorder.

4.2. Fragmentary vs. worm-like chain

To distinguish between a worm-like and a fragmentary chain, we would like to know if and how many abrupt changes occur in equilibrium conformations of the system. What defines an abrupt change may seem rather arbitrary, but our results are only weakly dependent of its absolute measure in the range of 10–30°. Crudely, one can think of bonds as completely conjugated ($\theta_i - \theta_{i+1} = 0$) or completely broken ($\theta_i - \theta_{i+1} = \pi/2$). We consider a slightly more realistic situation: an abrupt disruption is one in which $|\theta_i - \theta_{i+1}| > \alpha$. In our numerical studies, α was taken to be 10°, 15° and 20° without much qualitative difference.

Our model only includes nearest-neighbour interactions – the relative angles of double bonds are thus independent variables. The probability density distribution of any angle ϕ_i is

$$P(\phi) = \{\exp[\beta(E_c \cos 2\phi + E_s \cos \phi)]/Z\},$$

where

$$\beta = 1/kT$$

and

$$Z = \int_{-\pi}^{\pi} d\phi \exp(E_c \cos 2\phi + E_s \cos \phi).$$

For systems which favor a planar conformation, we expect the angles to be small, so we may expand the Hamiltonian around the minimum $\phi = 0$ (a similar approach can be taken for chains with a minimum configuration other than the perfectly planar one – no different qualitative behavior is expected),

$$H_R = \sum_{i=1}^{N} \Big\{-E_c[1 - 2(\phi_i)^2 - E_s\Big[1 - (\phi_i)^2/2\Big]\Big\}.$$

The probability density distribution now becomes

$$P(\phi) = \exp\{-\beta(\phi)^2(E_s + 4E_c)/2\} \Big/ \int_{-\pi}^{\pi} d\phi \exp\Big\{\Big[-\beta(\phi)^2\Big](E_s + 4E_c)/2\Big\}.$$

We can now obtain the probability of two adjacent double bonds being coplanar (i.e., $\alpha \approx 10$–$20°$) at room temperature, and we find it to be 0.75. From the numerical simulations, we also observe 70% of the angles to be in this range. Such clustering of the relative angles of double bonds around zero reenforces the fragmented chain picture. The most probable number of flips or breaks, $\langle m \rangle$, in the chain is given by

$$\langle m \rangle/N = \exp\{-(E_s + E_c)/kT\}.$$

E_s is directly related to V_0 and E_c to $\{t_d/t_s\}$. As the temperature T increases, we expect more flips to occur. Similarly a longer chain can support more

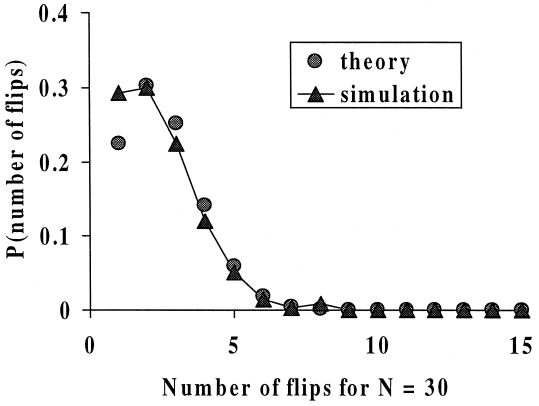

Fig. 7. Probability distribution of 'flips' in a chain of 30 carbons at $T = 300$ K from theory and simulations.

flips agreeing with our intuitive ideas. Also, at longer lengths, there is higher probability of conformational distortion. Additionally, we can infer from the above formula that as N increases, one expects to find more planar segments, instead of longer ones. So the distribution of lengths of the segments will eventually not depend on N.

More information regarding this model can be found in Yaliraki and Silbey [23], including analytic results for the probability distribution of flips and most probable number of flips. The final result of the model is a probability distribution of fully conjugated fragment of length λ in a chain of length N: $P^N(\lambda)$. If the probability of having two adjacent 'coplanar ' single bonds is p and the probability of their being 'non-coplanar' is $q = 1 - p$, then the probability of having λ coplanar single bonds in a chain of length $N > \lambda$ is $p^\lambda q$, since the next bond must be non-coplanar. Note that in our model coplanar means planar within an angle of α.

With these remarks on the expected conformational statistics of polyene chains, we now turn to numerical simulations of the chain using the Hamiltonian given above.

4.3. Numerical simulations

The effect of conformational disorder on conjugated systems and their absorption spectrum was also studied through numerical simulations. A Metropolis algorithm [50] was employed, choosing configurations weighted with a probability $\exp\{-\beta H\}$. Configurations were produced by flipping one angle at a time. From the equilibrium configurations, we extracted information about the manner of chain distortion. For the cases we considered, the notion of the fragmentary chain is realistic and well suited to the results.

We performed the simulations at three different temperatures, $T = 300$, 400 and 600 K, for five different ratios of transfer integrals t_s/t_d from 0.3 to 0.8, and for different values of the steric energy parameter V_0. First, we observed that the overwhelming majority of angles were indeed close to zero. We also looked for 'flips' and segments' in those chains with very good agreement to the predictions for the analytic model. This can be seen in Fig. 7. If we compare the values of the most probable number of flips for a chain of 30 atoms at different temperatures between predictions of the model and numerical simulations, we notice relatively good agreement. We see that the number of flips is substantial, supporting the idea of a fragmented chain.

4.4. Calculation of third-order polarizability

Using the model of a fragmentary chain, it is possible to calculate the value of the third-order polarizability, γ, in the following manner. We assume that the chain is fragmentary, that is broken into lengths of conjugated pieces separated by non-

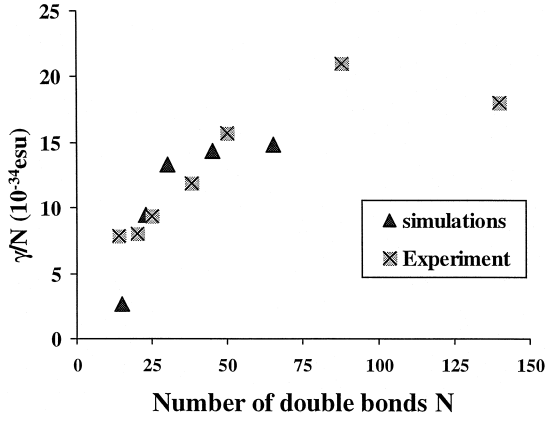

Fig. 8. Plot of $\gamma_{xxxx}(0)/N$ values from simulations and THG experiment.

conjugated pieces. Since we know the probability distribution of conjugated lengths, we assume that the total value of γ for a chain is the sum of the values for the conjugated segments. Thus, for a solution of chain molecules of length N, we can find the total number of conjugated segments, N_{tot}, and the probability distribution of finding a segment of length λ, $P^N(\lambda)$. Then if we know the third-order polarizability of a fully conjugated chain of length λ, $\gamma(\lambda)$, the polarizability of the ensemble is

$$\gamma = \sum \gamma(\lambda) N_{tot} P_N(\lambda) .$$

Using this formulation, Yaliraki and Silbey computed the value of γ/N for a solution of conjugated polyene molecules of length N double bonds. Results are sketched in Fig. 8, together with experimental data from Series I molecules.

5. Discussion

5.1. Linear absorption spectra

The observed λ_{max} or HOMO–LUMO transition energies for a given number of double bonds do not correspond to the values observed for unsubstituted polyenes [6]. This implies that the polymer is not fully planar and π orbital therefore do not fully overlap. The considerable blue-shift of absorption spectra of molecules from Series III with respect to those from Series I support the hypothesis of a severe limitation of the conjugation due to the presence of all 6-membered rings causing a steric hindrance, and then reducing the extent of electron delocalization. This is confirmed by the large difference in N_{eff} values for similar 'nominal' N's: in Series I, N_{eff} $(N = 50) = 15.3$, to be compared to N_{eff} $(49) = 10.5$ in Series III. Similarly, N_{eff} $(N = 88) = 17$ in Series I, to be compared to N_{eff} $(N = 86) = 11.4$ in Series III.

More detailed investigations have demonstrated that the distribution of effective conjugation lengths can be extracted from absorption spectra of solutions of Series I. These distributions are found to be dominated by short conjugation lengths [51].

The solvatochromic shift that is observed in Series III (see Fig. 3b) could be explained in terms of changes in polymer conformation in solvents of different dielectric constants. This strong sensitivity of the electronic structure to environment can play an important role in the limitation of conjugation in molecules from Series III.

5.2. Nonlinear optical properties

5.2.1. Comparison with previous calculations

Whereas the relative increase of γ and $\gamma(0)$ is almost 2 orders of magnitude as compared to shorter polyenes such as carotenoids or end-capped polynorbornene-polyenes, the enhancement is much lower for the hyperpolarizability per unit length γ/N, which is only 3 times larger than in the case of small polyene chains. The saturation effect experimentally reported for the first time in Ref. [22] is fully confirmed by the linear N-dependence of γ values for longer polyenes. It must be pointed out that a crude comparison of $\gamma(0)$ and $\gamma(0)/N$ values of different families of poyenes is not relevant. For example, the maximal value of $p = [\mathrm{d}\ln\gamma(0)]/[\mathrm{d}\ln N]$ of Series I molecules does not exceed 2, to be compared to the value $\alpha = 3.2$ of the exponent describing the power-law dependence of $\gamma(0)$ with respect to N ($\gamma(0) = kN^{\alpha}$) for the short model polyenes reported in Ref. [6]. Moreover, $\gamma(0)/N$ values for Series I molecules are 3 times higher than the corresponding ones for Series III at similar N values. Such discontinuities of linear and NLO properties between different types of polyenes suggest a strong influence of the chemical structure of the conjugated chain, that cannot be adequately modelized by purely electronic (e.g., Hückel-type) models. Results of previously reported modelling agrees qualitatively with the experimental behavior of $\gamma(0)$, $\gamma(0)/N$ and p. For example, a saturation of $\gamma(0)/N$ when increasing N is clearly demonstrated in a number of theoretical papers [26–28], as well as a maximal value of p, both depending on bond alternation δ. This δ-dependence appears to be much stronger in Ref. [27], so that it would be possible to find a δ value that gives the proper N_{sat} corresponding to saturation of γ, as well the adequate N_{max} corresponding to the maximum value of p. From figs. 3 and 4 from Ref. [27], it appears that for $\delta = 10^{-2}$, calculated $N_{max} = 55$ is significantly higher than for our experimental one ($N_{max} = 35$)

and calculated N_{sat} is significantly higher that its experimental equivalent. However, in the case of our molecules, no experimental evidence of $\delta = 10^{-2}$ is presently available, so that such comparisons between calculated and experimental data remain purely conjectural in terms of evaluation of bond alternation. Moreover, a quantitative comparison between calculated and experimental $\gamma(0)$ or $\gamma(0)/N$ values is problematic, units for γ being not clearly defined (except in Ref. [26] but in that case saturation is found to occur at much shorter conjugation lengths, etc.)

Of course, the discussion of experimental data would be made much easier when considering N_{eff} values instead of N ones. A plot of $\ln\gamma(0)$ with respect to N_{eff} for Series I shows a quasi-linear behavior, according to the power-law dependence $\gamma(0) = kN^{\alpha}$ observed in the case of short polyenes. But in the present case, the exponent α is very weak ($\alpha = 0.367$), one order of magnitude lower than in the case of 'model' polyenes or carotenoids reported in previous works.

5.2.2. Relevance of the present model

Such problems clearly suggest that the description of a given polyenic chain in terms of a single effective conjugation length is inadequate. As proposed in Ref. [23] and in this work, the chain is supposed to behave, not as one of smaller lengths than the nominal one, but as a collection of smaller ones. The model developed in the previous section points out as the relevant factor the probability distribution of the lengths of segments between large angular breaks. This factor may be strongly influenced by steric hindrances within the poyenic chain, so that even 'minor' structural changes within the conjugated backbone (e.g., by replacing alternate 5- and 6-membered rings by all 6-membered ones, as happens when comparing Series I and II or Series I and III) can significantly modify the optical properties of the molecule.

When we compare results from our model with experimental data, we immediately see on Fig. 8 that saturation is reached for chains of ~ 40 double bonds, longer than previous theoretical predictions for the fully planar all-*trans* molecules (~ 25 double bonds), and coming much closer to our experimental N_{sat} (~ 60). From that point of view, the present model brings a significant improvement in the description of the saturation behavior of γ's.

Moreover, the most important improvement arising from the present model is the clear evidence of a good quantitative agreement between calculated and experimental $\gamma(0)/N$ values for N ranging from 14 to 140 double bonds, provided that such a comparison is made on the same γ values. It must be pointed-out that the measured $\gamma(0;0,0,0) \equiv \gamma(0)$ value cannot be crudely compared to the calculated γ_{xxxx} ones [26], where x is the conjugation axis of polyenic molecules. In fact, the measured γ corresponds to an ensemble isotropic averaged value $\langle\gamma\rangle$ that can be developed in terms of the Cartesian components of the γ tensor according to:

$$\langle\gamma\rangle = \frac{1}{5}\left[\sum_i \gamma_{iiii} + \frac{1}{3}\sum_{i\neq j}\left(\gamma_{iijj} + \gamma_{ijji} + \gamma_{ijij}\right)\right]$$

where the indices i and j represent the Cartesian coordinates x, y, z. Considering the strong 1-D character of our molecules, we assume that γ_{yyyy}, γ_{zzzz} and all non-diagonal tensor components can be neglected with respect to γ_{xxxx}. Therefore, we have to plot in Fig. 8 the experimental $\gamma_{xxxx}(0) = 1/5\langle\gamma\rangle$, in order to be relevant with calculated γ's.

An excellent agreement is observed in terms of magnitudes of $\gamma_{xxxx}(0)/N$. A moderate discrepancy appears for larger N's, but never exceeds 25%. The experimental errors on both N and γ values being of the order of 10%, this agreement remains quite satisfactory. The validity of the present model is therefore clearly demonstrated when adequate γ values are compared to each other.

This model can be easily adapted to other families of polyene-like molecules, using a proper adjustment of the steric potential constant V_0 and of transfer integrals t_d and t_s. From Fig. 5 of Ref. [23], we clearly see the strong dependence of α/N (α being the linear polarizability) with respect to t_s (the magnitude of V_0 being in fact unimportant in that case). t_s strongly depends on experimental band gap E_g of the polyene, and decreases when E_g increases (for a given bandwidth W_g, see above). α/N dramatically falls down when t_s is reduced by a factor 1.414. A similar qualitative behavior being reasonably expected for γ, the much lower γ/N values observed

for Series III is actually correlated to the higher E_g and smaller t_s values.

The model of conformational defects that we have used was designed for unsubstituted polyenes (or oligomers of other simple conjugated systems), while the molecules that were synthesized and studied experimentally contained side groups, and 5- and 6-membered rings. In spite of this, the model gave good agreement with the experimental results, indicating that the essential parts of the physics of the problem are captured in the model. However, it should be noted that the agreement between experiment and theory is not perfect and, in particular, the theory predicts a faster saturation with N than does the experiment. This suggests that a more complete model that takes into account the effect of the side chains and the 5- and 6-membered rings might do a better job at describing the experiment. Such a model might have different torsional potentials along the chain, depending on the nature of the side group, etc.

6. Conclusions

The use of an alternative MALDI-TOF method for determination of molecular masses has evidenced a strong discrepancy with respect to values deduced from GPC viscometry. Molecular masses and N values must be reduced by a factor of 1.7 for Series I. This new molecular mass determination changes the saturation length as compared to experimental data reported in Ref. [22], then leading to more realistic N_{sat} values when comparing experimental data with calculated ones. It is clearly confirmed that the power-law dependence on N is a property of small polyenes – large polyenes have saturated values of polarizabilities with variable exponents values that exhibit a maximum around $N_{max} = 35$ for our molecules. The model proposed here takes into account the important role of rotations around single bonds, and provides quantitative data that may be directly compared to experiment ones, providing that the tensorial character of γ is taken into account. In these conditions, a very good quantitative agreement is found for both saturation lengths and $\gamma(0)/N$ values, then validating this model for an accurate description of the linear and NLO properties of 1-D conjugated chains.

Acknowledgements

The authors thank Dr. Heinz Köchling and Professor Klaus Biemann for obtaining MALDI-TOF spectra. They also thank Corinne Delporte for help in THG solution measurements. The work of Yaliraki and Silbey was supported by the National Science Foundation under a MRSEC grant 9400334. RRS thanks the Director, Office of Basic Energy Research, Office of Basic Energy Sciences, Chemical Sciences Division of the US Department of Energy (Contract DE-FG02-86ER13564) for support.

References

[1] H. Naarman, N. Theophilou, Synth. Met. 22 (1987) 1.
[2] J.H. Burroughs, D.D.C. Bradley, A.R. Brown, R.N. Marks, K. Mackay, R.H. Friend, P.L. Burns, A.B. Holmes, Nature (London) 347 (1990) 539.
[3] N.C. Greenham, S.C. Moratti, D.D.C. Bradley, R.H. Friend, A.B. Holmes, Nature (London) 365 (1993) 628.
[4] K.C. Rustagi, J. Ducuing, Opt. Commun. 10 (1974) 258.
[5] G.P. Agrawal, C. Cojan, C. Flytzanis, Phys. Rev. B 17 (1978) 776.
[6] G.S.W. Craig, R.E. Cohen, R.R. Schrock, R.J. Silbey, G. PUccetti, I. Ledoux, J. Zyss, J. Am. Chem. Soc. 115 (1993) 860.
[7] G. Puccetti, M. Blanchard-Desce, I. Ledoux, J.-M. Lehn, J. Zyss, J. Phys. Chem. 97 (1993) 9385.
[8] J.F. Ward, D.S. Elliott, J. Chem. Phys. 69 (1978) 5438.
[9] S.R. Marder, J.W. Perry, F.L. Klavelta, R.H. Grubbs, Chem. Mater. 1 (1989) 171.
[10] J.P. Hermann, D. Ricard, J. Ducuing, Appl. Phys. Lett. 23 (1973) 178.
[11] B.E. Kohler, C.W. Spangler, C. Westerfield, J. Chem. Phys. 89 (1988) 5422.
[12] A.J. Heeger, S. Kivelson, J.R. Schrieffer, W.P. Su, Rev. Mod. Phys. 60 (1988) 781.
[13] C.V. Shank, R. Yen, R.L. Fork, J. Orenstein, G.L. Baker, Phys. Rev. Lett. 49 (1982) 1657.
[14] E.F. McIntyre, H.F. Hameka, J. Chem. Phys. 68 (1978) 3481.
[15] D.N. Beratan, J.N. Onuchic, J.W. Perry, J. Phys. Chem. 91 (1987) 2696.
[16] Z. Soos, S. Ramasesha, J. Phys. Chem. 90 (1989) 1067.
[17] J. Heflin, K. Wong, O. Zamani-Khamiri, A. Garito, Phys. Rev. B 38 (1988) 1573.
[18] C.P. de Melo, R.J. Silbey, Chem. Phys. Lett. 140 (1987) 537.
[19] H.H. Fox, R.R. Schrock, Organometallics 11 (1992) 2763.
[20] H.H. Fox, J.K. Lee, L.Y. Park, R.R. Schrock, Organometallics 12 (1993) 759.
[21] H.H. Fox, M.O. Wolf, R. O'Dell, B.L. Lin, R.R. Schrock, M.S. Wrighton, J. Am. Chem. Soc. 116 (1994) 2827.
[22] D.W. Samuel I, I. Ledoux, C. Dhenaut, J. Zyss, H. Fox, R.R. Schrock, R.J. Silbey, Science 265 (1994) 1070.

[23] S.N. Yaliraki, R.J. Silbey, J. Chem. Phys. 104 (1996) 1245.
[24] Z.G. Soos, K.S. Schweitzer, Chem. Phys. Lett. 139 (1987) 196.
[25] J.O. Morley, V.J. Docherty, D. Pugh, J. Chem. Soc., Perkin Trans. 2 (1987) 1351.
[26] D. Yaron, R.J. Silbey, Phys. Rev. B 45 (1992) 11655.
[27] F.C. Spano, Z.G. Soos, J. Chem. Phys. 99 (1993) 9265.
[28] H.X. Wang, S. Mukamel, Nonlin. Opt. 5 (1993) 281.
[29] F.J. Schattenmann, R.R. Schrock, W.M. Davis, J. Am. Chem. Soc. 118 (1996) 3295.
[30] F.J. Schattenmann, R.R. Schrock, Maromolecules 29 (1996) 8990.
[31] G. Wilczek-Vera, P.O. Danis, A. Eisenberg, J. Am. Chem. Soc. 118 (1996) 4036.
[32] H. Pasch, F. Gores, Polymer 36 (1995) 1999.
[33] D.R. Maloney, K.H. Hunt, P.M. Lloyd, A.V.G. Muir, S.N. Richards, P.J. Derrick, D.M. Haddleton, J. Chem. Soc., Chem. Commun. 561 (1995) .
[34] D.R. Maloney, K.H. Hunt, P.M. Lloyd, A.V.G. Muir, S.N. Richards, P.J. Derrick, D.M. Haddleton, J. Chem. Soc., Chem. Commun. 561 (1995) .
[35] P. Juhasz, C.E. Costello, K. Biemann, J. Am. Soc. Mass Spectrom. 4 (1993) 399.
[36] P.O. Danis, D.E. Karr, W.J. Simonsick, D.T. Wu, Macromolecules 28 (1995) 1229.
[37] A. Szabo, J. Langlet, J.-P. Malrieu, Chem. Phys. 13 (1976) 173.
[38] M. Sinclair, D. Moses, K. Akagi, A.J. Heeger, Phys. Rev. B 38 (1988) 10724.
[39] C. Halvorson, T.W. Hagler, D. Moses, Y. Cao, A.J. Heeger, Chem. Phys. Lett. 200 (1992) 364.
[40] Z. Shuai, J.-L. Brédas, Phys. Rev. B 44 (1991) 5962.
[41] J. Yu, W.P. Su, Phys. Rev. B 44 (1991) 13315.
[42] G. Rossi, A. Viallat, Phys. Rev. B 40 (1989) 10036.
[43] G. Rossi, A. Viallat, J. Chem. Phys. 92 (1990) 4548.
[44] P. Pincus, G. Rossi, M.E. Gates, Europhys. Lett. 4 (1987) 41.
[45] R. MacKenzie, J.M. Ginger, A.J. Epstein, Phys. Rev.B. 44 (1991) 2362.
[46] J.L. Bredas, C. Quattrochi, J. Libent, A.C. MacDiarmid, J.M. Ginger, A.J. Epstein, Phys. Rev. B. 44 (1991) 6002.
[47] L. Salem, The Molecular Orbital Theory of Conjugated Molecules, Benjamin, New York, 1966.
[48] W.P. Su, J.R. Schrieffer, A.S. Heeger, Phys. Rev. B 22 (1980) 2099.
[49] G. Rossi, R.R. Chance, R.J. Silbey, J. Chem. Phys. 90 (1989) 7594.
[50] N. Metropolis, A.W. Rodenbluth, M.N. Rosenbluth, A.H. Teller, E. Teller, J. Chem. Phys. 21 (1953) 1087.
[51] B.E. Kohler, I.D.W. Samuel, J. Chem. Phys. 103 (1995) 6248.